ORIGINAL ARTICLE

Tool path pattern and feed direction selection in robotic milling for increased chatter-free material removal rate

L.T. Tunc[1] · Dave Stoddart[1]

Abstract Robotic milling becomes increasingly relevant to large-scale part manufacturing industries thanks to its cost-effective and portable manufacturing concept compared to large-scale CNC machine tools. Integration of milling processes with industrial robots is proposed to be well aligned with the aims and objective of the recent fourth industrial revolution. However, the industrial robots introduce position-dependent and asymmetrical dynamic flexibility, which may reflect to the tool tip dynamics under several conditions. Under such circumstances, the stability limits become dependent on the machining location and the feed direction. In this respect, selection of machining tool path patterns is crucial for increased chatter-free material removal rates (MRR). This paper proposes an approach to evaluate and select tool path patterns, offered by the existing CAM packages, for increased chatter-free MRR. The machining area is divided into number of machining locations. The optimal feed direction is decided based on the absolute stability at each region considering the asymmetrical and position-dependent tool tip dynamics. Then, the alternative tool path patterns are evaluated and the corresponding optimum feed direction is decided for increased chatter-free material removal. The application of the proposed approach is demonstrated through simulations and representative experiments.

Keywords Robotic milling · Stability · Machining strategy

✉ L.T. Tunc
    taner.tunc@namrc.co.uk; tanertunc@sabanciuniv.edu

[1] Nuclear Advanced Manufacturing Research Centre, University of Sheffield, Sheffield, UK

1 Introduction

The use of robots for machining processes has been increasing for the last decades [1]. Robotic milling is one of the relevant technologies especially for large-scale part manufacturing industries, where successful use proposes significant cost reduction. Chatter is the major limitation in milling operations [2, 3], which can be avoided by identifying the stable cutting conditions through analysis and simulation of milling dynamics and stability [2]. Stable cutting conditions are governed by dynamic response of the system at the tool tip, which is a coupled response of the modes contributed by the structure of the machining unit, spindle, tool holder, tool, and sometimes the workpiece. In a recent study, it was shown that the coupling between multiple dominant modes might lead to important variations in stability diagrams [4]. As the flexible dynamics of the robotic structures are considered, robotic milling can be considered as a candidate for such a case based on the tooling condition. In robotic milling applications, it has been previously identified that the tool tip dynamics may become asymmetrical and position dependent due to the asymmetrical modes contributed by the flexible structure of the robot in feed, cross feed, and spindle axis directions [5, 6]. The asymmetrical tool tip dynamics introduces a feed direction effect on the stability diagrams, i.e., stable cutting conditions. Thus, the machining tool path pattern becomes an important parameter for increased chatter-free material removal rates in robotic milling. This paper presents a new machining tool path selection approach, which considers such effects.

In high-value manufacturing industries, selection of the tool path pattern is very crucial to achieve the desired productivity and part quality, which currently relies on the default templates offered by the CAM modules. This topic has been studied by several authors either experimentally or using process modeling and simulation techniques. In an early study on

machining strategy selection, Feng and Su [7] studied and integrated the approach for selection of feed direction and feed rate velocity for 3D plane surfaces. They showed that the shortest tool path length does not always result in maximum efficiency due to the feed rate velocity limitations. They also stated that the optimum cutter feed direction is in general not unique but falls within an optimum range in the finish machining of 3D plane surfaces. Ramos et al. [8] put an experimental effort to compare the effect of tool path patterns such as radial, raster, and 3D offset on surface quality in free-form surface machining. They found out that the machining times did not differ significantly among the machining strategies applied on machining of the naval type impeller geometry. However, the 3D offset strategy was found out to be the most suitable pattern for best surface finish and best dimensional control performance. Toh [9] studied the effect of feed direction in three main tool path patterns, i.e., offset, raster, one-direction raster, entrance and exit angles of the cutter, and inclined milling effects. In this study, general guidelines in selection of feed direction leading to minimum tool path length for different tool path patterns are derived. It was also stated that machining with an inclination angle of 15° results in better surface quality and tool life in ball end milling. Monreal and Rodrigues [10] also studied the influence of tool path strategy on the actual cycle time at high-speed milling conditions. They analyzed different feed direction angles with raster type tool paths and predicted the discrepancy between the programmed feed rate velocity and the actual feed rate velocity due to the machine tool acceleration and deceleration. Their predictions supported that intelligent selection of the feed direction plays a significant role in achieving decreased actual cycle times.

In surface finish machining applications, it is important to apply a tool path pattern compatible with the surface characteristics for improved surface quality. Giri et al. [11] proposed an approach to select the machining strategy in three-axis free-form surface milling by clustering the feed directions based on the intrinsic properties of the surface such as curvature so that the cutting tool traverse direction was kept compatible with the surface characteristics. Quinsat et al. [12] studied optimal selection of machining tool path strategies in three-axis ball end milling of sculptured surfaces in a similar perspective. They considered the intrinsic properties of the surface contrary to the conventional iso-scallop strategy in the selection of the tool path pattern, i.e., master cutter path, for sculpture surface machining. They introduced directional beams, related to the local surface parameters, to represent the set of feed directions for guaranteed maximum performance. Later, Bohez et al. [13] extended this approach to five-axis milling by using the normalized cut clustering technique to partition the vector fields.

With the developments in process modeling and simulation capabilities, the selection of the milling tool path pattern considering the process mechanics gained more importance, where cutting forces and tool deflection were taken into account. Several authors dealt with this issue based on milling mechanics and surface quality where cutting forces, tool deflections, maximum feed rate maps, and surface texture are utilized to decide feed direction and select the best tool path pattern. In an early study, Lim and Menq [14] proposed an algorithm for selection of the best local cutting directions, where various cutting directions at each cutter location were compared according to the cutting forces. The maximum feed rate map is also generated using cutting force simulations. Lacalle et al. [15] determined local machining directions minimizing the tool deflection at a given cutter location for better dimensional quality. Later, Lazoglu et al. [16] extended the process simulation-based tool path optimization approach on five-axis milling cycles by proposing a tool path pattern optimization approach considering multi-objectives bound to cutting forces. They selected and compared the optimized tool path pattern for a minimum cost traveling salesman, a minimum spanning tree, and minimum cost connections. They showed that free-form surface finishing tool paths can be optimized for less variation in cutting forces with decreased peak values. Then, this methodology is extended to a multi-criteria optimization approach [17], where cutting forces, cycle time, and scallop height were considered as objectives.

In the last decades, the robotic machining concept has been tremendously increasing. Several authors assessed industrial robots to be employed in machining tasks. The main areas of research have been focused on chatter analysis and vibration response [18, 19] modeling the structural stiffness [20], feed rate, and motion planning [21]. In these studies, it is mentioned that the industrial robots introduce asymmetrical and position-dependent dynamic response to the machining system. This, in return, causes the tool tip dynamics to become significantly position-dependent and asymmetrical in feed and cross-feed directions [5]. For such cases, the stable cutting conditions depend on the feed direction, as well as even in simple end milling conditions [6]. As a result, it is fair to conclude that the machining tool path pattern becomes an important parameter for the stable cutting conditions considering that the feed direction is decided by the applied tool path pattern. In this regard, this paper proposes an approach to take into account such significant variations in the dynamic response of robotic milling systems in the selection of the tool path pattern for an increased chatter-free material removal rate. The proposed approach acquires the tool tip frequency response function (FRF), either by simulations or measurements, at various machining locations among the machined areas. Then, at each machining location, the preferable machining direction is selected based on process stability. Finally, the machining

directions are clustered to generate an organized tool path. The currently available machining tool path patterns are rated with respect to the optimized feed directions, where the absolute stability index (ASI) and the maximum stability index (MSI) are introduced. Henceforth, the paper is organized as follows: the robotic machining setup used in the experiments is explained in the next section. This is followed by a brief analysis of the dynamic response of the robotic machining focusing on the effect of the asymmetrical tool tip FRF on the feed direction-dependent stability. The stability-based tool path pattern selection and evaluation are given in Section 5; the paper is finalized with case studies and representative experiments in Section 6 together with conclusions and outlook.

2 Robotic machining unit

The simulations and experiments are performed considering the dynamics of the robotic milling system, which consists of a Fanuc F200iB six degrees of freedom parallel kinematic hexapod robot controlled by a Fanuc R-30iA controller. The hexapod platform is fitted with an 8-kW spindle (see Fig. 1), which can run at a maximum spindle speed of 6000 rpm. The allowable payload and load moment on the robot are 100 kg and 60 kgfm, respectively. Such a load capacity enables light- or medium-duty milling operations to be carried out. The links of the robot can provide maximum feed rate values of 18 and 90 m/min in vertical (Y-axis) and horizontal (X-Z plane) directions, respectively.

Robot programming is performed in the following manner: the reference point of the workpiece is defined to the robot as a user frame, whereas the tool center point is taught as a tool frame with respect to the global frame of the robot. The cutter pass control is performed b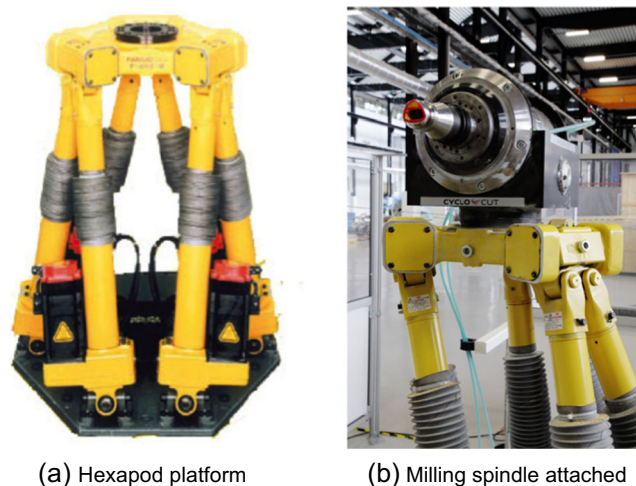y converting the cutter location file into series of linear motion commands recognized by the robot, where the tool path is generated using Siemens NX9 ©.

3 Milling stability

The equations of motion for a two-DOF milling system need to be written in feed and cross-feed directions after the frequency response functions in X and Y directions are measured in the global robot coordinates, i.e., X and Y. It is noteworthy to emphasize that once the frequency response functions are measured along the X, Y directions, the projection of them along the feed and cross-feed directions is performed through vector algebra, which are the principal excitation directions. In general, the cutter feed rate direction can be at any angle, φ, with respect to the X direction of the robot as illustrated in Fig. 2. One can write the oriented frequency response functions as follows:

$$
\begin{aligned}
G_f &= G_{xx}\cos\varphi + G_{yy}\sin\varphi \\
G_{cf} &= -G_{xx}\sin\varphi + G_{yy}\cos\varphi
\end{aligned}
\tag{1}
$$

The oriented frequency response functions are used in the stability solution after writing the dynamic forces and displacements in the frequency domain [22]. In Eq. (2), $G(i\omega_c)$ is the matrix holding the direct and cross-frequency response functions in feed and cross-feed directions.

$$
\{F\}e^{i\omega_c t} = \frac{1}{2}aK_t\left(1-e^{-i\omega_c T}\right)\underbrace{[A_0][G(i\omega_c)]}_{[G_0(i\omega_c)]}\{F\}e^{i\omega_c t}
\tag{2}
$$

The stability of the above frequency domain equation reduces to an eigenvalue problem considering that it has a nontrivial solution only if its determinant is zero [22]:

$$
\det[[I] + \Lambda[G_0(i\omega_c)]] = 0
\tag{3}
$$

(a) Hexapod platform   (b) Milling spindle attached
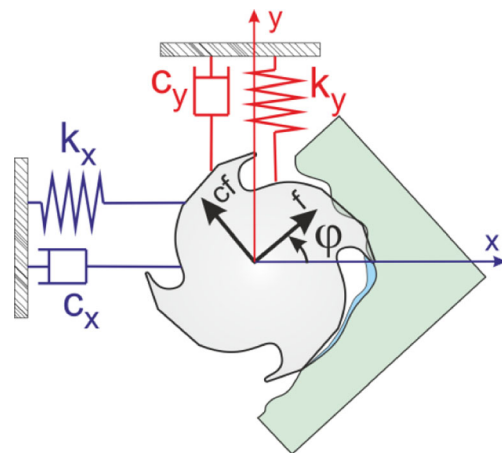
Fig. 1 Robotic machining unit

Fig. 2 End milling system with oriented frequency response functions

The eigenvalue, Λ, of Eq. (3) is written in terms of process parameters:

$$\Lambda = -\frac{N}{4\pi} K_t a \left(1 - e^{-i\omega_c T}\right) \qquad (4)$$

Finally, the limiting stable cutting depth for the end milling system is obtained by writing the eigenvalue, Λ, in terms of the frequency response functions:

$$a_{\lim} = -\frac{2\pi \Lambda_R}{NK_t} \left(1 + \kappa^2\right)$$
$$\text{where } \Lambda = -\frac{1}{2a_0} \left(a_1 \pm \sqrt{a_1^2 - 4a_0}\right) \qquad (5)$$

In Eq. (5), Λ_R is the real part of the eigenvalue Λ. κ is the ratio between the imaginary and the real part of the eigenvalue, which is also written in terms of the chatter frequency, ω_c, and the tooth-passing period, T. In the stability solution proposed by Altintas and Budak [22], a_0 and a_1 are written in terms of the direct frequency response functions of the system, G_{xx}, G_{yy}, and the average directional coefficients α_{xx}, α_{yy}, α_{xy}, and α_{yx}, which are functions of the start and exit angles, and the radial cutting force coefficient. The readers should be notified that in the proposed stability solution, xx and yy are referred to as the feed and cross-feed directions, respectively. Therefore, the stability of symmetrical milling systems is not affected by the feed direction as the oriented frequency response functions in Eq. (1) will not change with feed direction. However, the stability of asymmetrical systems such as milling robots will be affected by the feed direction as discussed in the rest of this paper.

4 Dynamics of the robotic machining unit

The machining setup involves a parallel kinematic mechanism (PKM) as being a hexapod robot. Law et al. [23] mentioned the difficulties in modeling of the joint dynamics, which complicates the modeling efforts to simulate the dynamics of PKM involved machining units such as the hexapod robot. Thus, considering the potential accuracy issues regarding the natural frequencies, and amplitude of the dynamic response at the tool tip, in this study, the frequency response function (FRF) is experimentally measured using impact hammer testing rather than simulation. Nonetheless, one can integrate the proposed approach with proper simulation models, which can predict the tool tip dynamics with the effect of the robotic structure. In this section, representative measurements are discussed to demonstrate how the robotic structure affects the tool tip dynamics in terms of position dependency, asymmetrical behavior, and the ratio of the FRF amplitudes in X and Y directions.

4.1 Position-dependent dynamics at the tool tip

The dynamic response at the tool tip results from coupling between the robot, the spindle, the tool holder and the cutting tool body. Thus, any change in any one of these components would result in variation in the tool tip dynamics. In this specific robotic milling application, the dynamic response of the hexapod robot significantly varies with the machining location due to changing lengths and angles of the six struts making up the PKM assembly, which would result in variation of the tool tip dynamics under certain tooling conditions. The aforementioned position dependency of the robotic milling setup is assessed by measuring the dynamic response at the tip of a long and slender milling tool having 16 mm diameter and 160 mm length, at 30 positions of the robot within a 2D working envelope of 300 mm × 300 mm, as shown in Fig. 3.

The plotted FRFs in Fig. 3b, c show that the dynamic response at the tool tip may significantly vary with the robot position. The low-frequency modes introduced by the hexapod robot in X and Y directions vary from 50 to 60 Hz, and from 120 to 130 Hz, respectively. Consequently, the modes introduced by the cutting tool body, at relatively higher frequencies, vary in terms of the amplitudes and the natural frequencies. Observing the modes at low frequency ranges, another important conclusion derived from Fig. 3 is that the robot introduces asymmetrical dynamics in principal directions of the tool. The detailed analysis of the position dependency can be found in a previous work of the authors [5, 6].

4.2 Asymmetrical tool tip dynamics

The dynamics of the robotic base is significantly asymmetrical in X and Y directions as plotted in Fig. 4a. The asymmetrical modes contributed by the robot lead the higher-frequency modes to become asymmetrical as well. Because of such a significant asymmetry, the feed direction becomes significantly important for the stable cutting conditions. Henceforth, this section discusses the effect of the asymmetrical dynamic response at the tool tip on selection of the feed rate direction and evaluation of machining tool path strategies.

Figure 4a shows that the dynamic response at the tool tip in the X direction varies as the robot moves from position 1 to position 25; however, the dynamic response in the Y direction does not show such a significant variation. The stability diagrams depend on the oriented frequency response functions along the feed, Gf, and cross-feed directions, Gcf. Thus, variation of the ratio between G_{xx} and G_{yy} from position 1 to position 25 will lead to different optimum feed directions while the robot is machining at the vicinity of these positions. Figure 4b shows the variation of the peak amplitude of Gf with the feed angle φ at position 1 and position 25. The feed rate direction, leading to the

Fig. 3 Position-dependent tool tip FRF in 2D work envelope. **a** Robot positions. **b** G_{xx} vs Y movement of the robot. **c** G_{yy} vs Y movement of the robot

(a) Robot positions

(b) Gxx vs Y movement of the robot

(c) Gyy vs Y movement of the robot
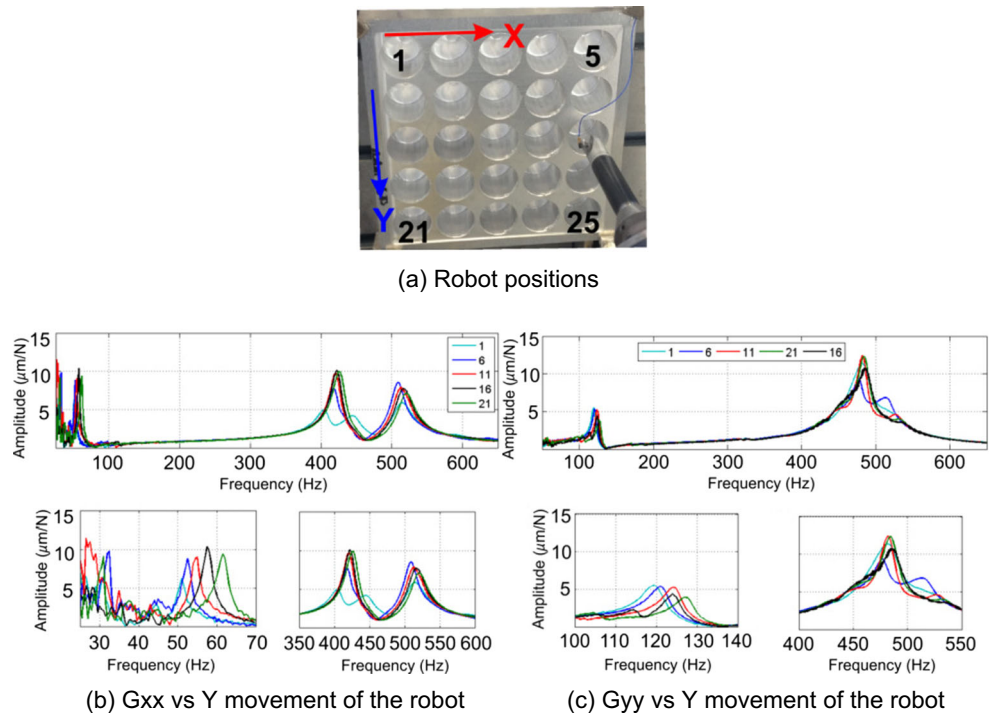
minimum peak amplitude of the dominant mode in the oriented frequency response function, would result in maximum stability. For instance, in Fig. 4b, the minimum peak amplitude of the oriented frequency response function in feed direction is minimized for the feed angle of 0° and 40°, at robot position 1 and robot position 25, respectively. Thus, it can be concluded that the variation of the ratio between G_{xx} and G_{yy} significantly affects the optimum feed rate direction for increased stability, where G_{xx} and G_{yy} are the frequency response functions measured in the global X and Y-axes of the robot.

Figure 5 shows the variation of the ratio between G_{xx} and G_{yy} with robot position, for the representative cutting tool used in this example. It is observed that the G_{xx} to G_{yy} ratio significantly varies with the robot position, both at low frequencies and at high frequencies. For instance, the

higher-frequency mode introduced by the cutting tool becomes more flexible in the X direction with respect to the Y direction as the robot gradually moves from position 1 to position 21. The amplitude of G_{xx} with respect to G_{yy} is 2 when the robot is at position 1, which increases up to 3 when the robot goes to position 21. This is an important observation in order to understand how the optimum feed rate direction would be affected by the asymmetrical and position-dependent dynamics introduced by the robotic platform.

5 Stability-based tool path selection

The previous sections discussed the variations in the tool tip dynamics with the effect of the robotic platform, which

Fig. 4 Asymmetrical tool tip FRF. **a** Effect of robot position. **b** Variation of peak amplitude in feed direction
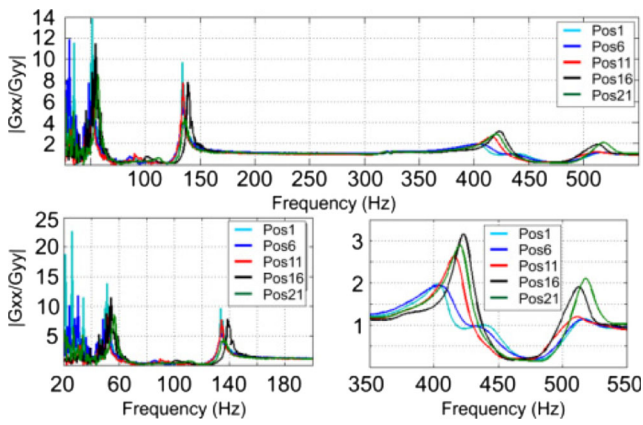

(a) Effect of robot position

(b) Variation of peak amplitude in feed direction
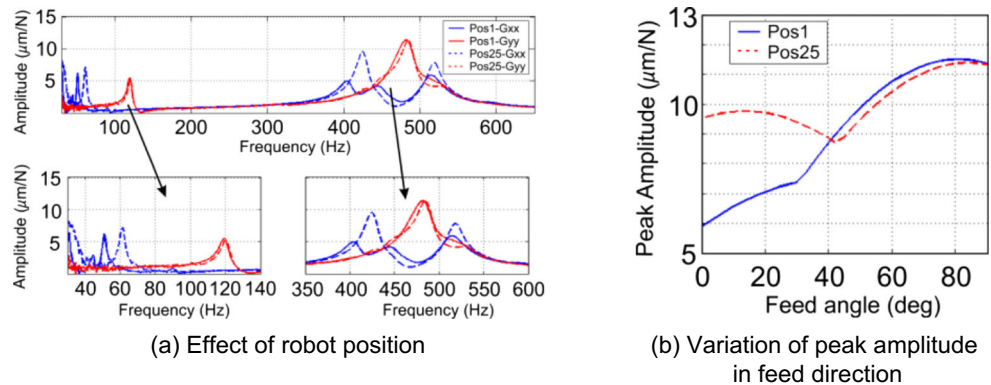
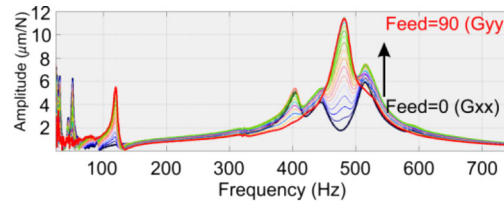**Fig. 5** Variation of G_{xx}/G_{yy} with robot position

significantly affects the preferable feed direction for increased stability in robotic milling. Henceforth, this section presents the algorithm developed to select the tool path pattern. Initially, the effect of feed direction on stability diagrams is discussed, which is followed by the determination of the preferable feed direction and evaluation of a given milling tool path pattern.

5.1 Effect of feed direction on stability limits

The tooling case given in Section 4 is considered to demonstrate the effect of the feed rate on the stability diagrams. The frequency response functions G_{xx} and G_{yy} are measured at position 1 and position 25, where the robot is located at the $Z = -100$ mm plane with respect to its reference frame. Then, G_{xx} and G_{yy} are oriented in feed and cross-feed directions for feed angles varying from 0° to 90°, which are used in simulation of the stability diagrams for varying feed directions. The oriented frequency response functions in feed direction, at position 1 of the robot, are plotted in Fig. 6a, where it gradually diverges from G_{xx} to G_{yy} as the feed angle is varied from 0° to 90°. The stability diagrams are generated for 18° of feed angle increments, for half immersion down milling of AL7075 material with average cutting force coefficients of Kt = 800 MPa and Kr = 300 MPa.

Figure 6b shows that the stability diagram varies with the feed direction in terms of both absolute stability and location of the stability lobes. In this specific case, the maximum absolute stability limit is observed around 0.6 mm when the feed direction is in 90°, i.e., cutting along the Y direction. However, as the stability lobes are concerned, there is a large common

Fig. 6 Effect of feed direction on stability limits. **a** Variation of the feed direction-oriented frequency response function. **b** Variation of stability diagrams with feed direction at position 1. **c** Variation of optimum feed direction with robot position
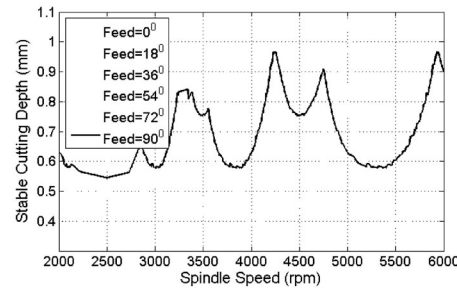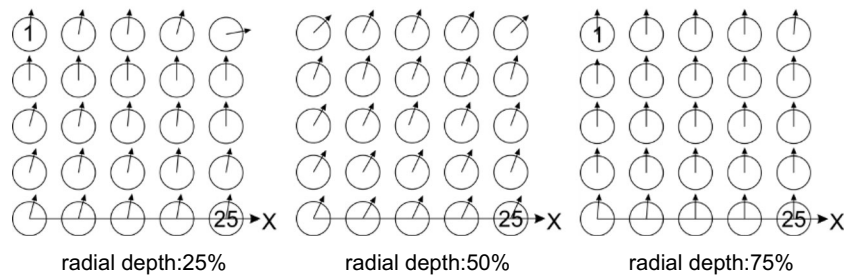

(a) Variation of the feed direction oriented frequency response function.

(b) Variation of stability diagrams with feed direction at position 1.

(c) Variation of optimum feed direction with robot position.

region of stability lobes for varying feed directions around 5000 rpm. It means that increased stability can be achieved by either adjusting the feed direction or setting the spindle speed accordingly.

In this study, the effect of the feed rate direction and hence selection of the machining tool path pattern is proposed for an *XY* plane, where the *Z* location of the robot is known by the workpiece geometry. The variation of the dynamic response with a limited positional change of the robot in the *Z* direction is ignored assuming that the robot moves in a range of 20 mm along the *Z* direction, for planar cuts. However, it should be kept in mind that if the robot's *Z* location with respect to the workpiece is to be decided, the dynamics and stability of the robot should be considered in a 3D volume as detailed in a previous study of the authors [5].

5.2 Determination of the optimum feed direction and evaluation of milling tool path patterns

The feed direction significantly affects both the absolute stability limit and the location of possible common stability pockets. In this regard, the feed direction leading to the maximum absolute stability limit may not lead to the maximum stability limit within the common stability pocket for all robot positions. Therefore, in this study, the optimum selection of feed direction is considered both in a local and a global manner. The local optimum feed direction is considered to evaluate a milling path pattern in terms of absolute stability limit, whereas the global optimum feed direction is considered in terms of the maximum stability limit for the common stability pockets.

Calculation of the stability diagram requires the radial depth of cut to be known, which affects the optimum feed direction due to the directional coefficients. The effect of the radial depth of cut on the maximum chatter-free cutting conditions was previously studied by Budak and Tekeli [24], where a procedure to select the radial depth of cut leading to maximum chatter-free material removal rates was proposed. Thus, it is noteworthy to state that selection

of the radial depth of cut should be performed priorly due to its effect on the local and global optimum feed rate directions. For this specific case, the optimum feed directions are selected for radial depth of cut values of 25%, 50%, and 75% of the tool diameter as shown in Fig. 6c, at 25 distinct locations of the robot (see Fig. 3a). It is seen that the preferable feed direction for increased absolute stability varies with both robot position in the same *XY* plane and the radial depth of cut.

CAM packages offer several default milling tool path patterns such as "zig," "zig-zag," and "follow periphery" as illustrated in Fig. 7. In the zig pattern, the feed direction is set and all the tool path lines are parallel to each other while keeping the same cutting mode, either down or up milling. In the zig-zag pattern, the feed direction is set and the rest of the tool path lines are parallel to each other but the cutting mode is altered between down milling and up milling. In either the zig or the zig-zag pattern, a single feed direction can be selected along any direction. In the follow periphery pattern, the cutting mode is kept constant but the feed direction is varied from 0° to 90° with respect to the *X*-axis.

The local feed rate directions are governed by the selected tool path pattern. Thus, milling stability should be considered using the local feed directions as the robot moves throughout the workspace. As continuous tracking of the variation of the positional-dependent dynamics at the tool tip is not practical, the area covered by the tool path is discretized into the number of points, where the dynamics and stability of the process are assessed. Then, the candidate tool path patterns are evaluated according to the achievable absolute stability limit as summarized in Fig. 8, where the absolute stability index, i.e., ASI, is calculated as follows:

$$\text{ASI} = \sum_{p=1}^{N} \frac{a_{\text{abs}}^{p}}{a_{\text{abs,opt}}^{p}} \tag{6}$$

In Eq. (6), p is the corresponding local point index; N is the total number of local points, a_{abs}^{p} is the absolute stability limit obtained at point p, along the feed direction

Fig. 7 Default tool path patterns offered by CAM packages. **a** Zig pattern. **b** Zig-zag pattern. **c** Follow periphery pattern

(a) zig pattern

(b) zig-zag pattern

(c) follow periphery pattern
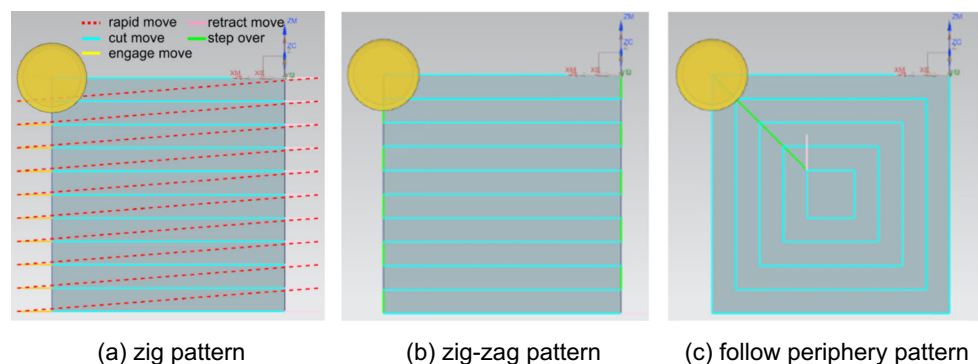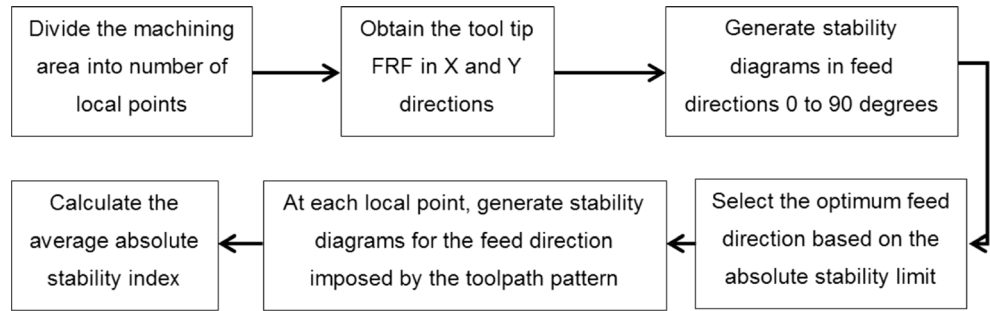
imposed by the tool path pattern; and $a_{\text{abs,opt}}^{p}$ is the absolute stability limit obtained along the optimum feed direction.

6 Case study

This section demonstrates the application of the proposed approach for milling tool path pattern selection in a pocketing operation for an increased chatter-free material removal rate. In the first simulation study, the local and global optimum feed directions are selected, whereas in the second study, the default milling tool path patterns are compared with respect to the absolute stability index. Then, the results are verified through representative experiments in Section 6.2.

6.1 Simulations

6.1.1 Selection of the local and global optimum feed directions

The case study involves milling of an AL7075 part having pocket dimensions of 300 mm × 300 mm × 20 mm. The radial depth of cut and the cutting mode are selected as 50% and down milling, respectively. A 25-mm-diameter end mill with two cutting inserts is used (see Fig. 3a). In this specific case, the robot is at $Z = -300$ mm plane with respect to its global reference frame. The machining area is divided into 49 distinct points (7 along width × 7 along height) at those the tool tip FRF is measured. The distance between the measurement positions is selected as double of the tool diameter, i.e., 50 mm. In order to smooth the variation of feed directions, a near-

Fig. 9 Selection of optimum/ near-optimum feed directions. **a** Variation of stability limits with feed direction (position 38). **b** Absolute stability optimal local feed directions. **c** Overall stability diagrams
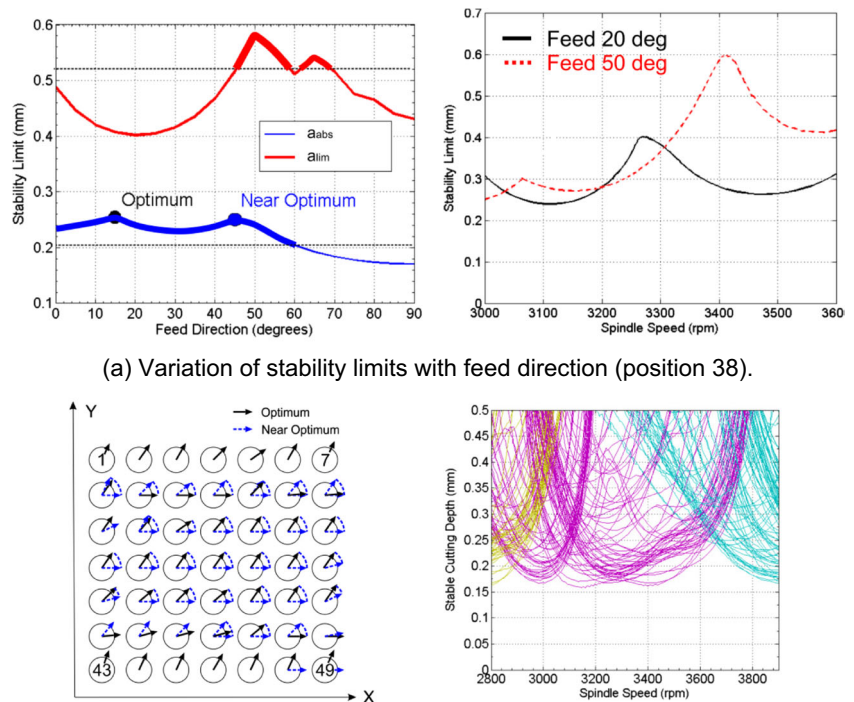
(a) Variation of stability limits with feed direction (position 38).

(b) Absolute stability optimal local feed directions

(c) Overall stability diagrams.

optimum feed direction is defined for the points whose optimum direction seems to be an outlier. A feed direction is nominated as near optimum if the corresponding absolute stability limit is within a 10% tolerance with respect to that of the optimum feed direction. The nominal cutting speed is selected as 260 m/min considering the dry cutting of AL7075, which corresponds to a spindle speed around 3300 rpm. However, considering the lobbing effect, the stability diagrams are calculated for the spindle speed range of 2800 to 3800 rpm.

At position 38, the variation of the absolute stability limit, i.e., a_{abs}, and the max stability limit around the 3300-rpm lobe, i.e., a_{lim}, with the feed rate direction are plotted in Fig. 9b. It is seen that 15° of feed direction is in terms of the absolute stability limit; however, the near-optimum feed direction range is quite wide up to 60°. As the maximum stability limits at the stability pocket around 3300 rpm are considered, the feed direction of 50° seems to be optimal and the range from 45° to 70° can be considered as near optimum. The selection procedure is performed similarly for other robot positions, where the optimum feed direction and the range of near-optimum feed directions based on the absolute stability limit are plotted in Fig. 9b. The stability diagrams calculated at each robot position along the local optimum feed directions are plotted in Fig. 9c.

In Fig. 9b, the absolute stability optimal feed directions are depicted as smoothly varying within a feed angle range from 40° to 55° except some outliers. However, as the near-

optimum feed directions are considered, the outliers are smoothed to fit in the general feed angle range from 45° to 55°. Thus, it can be concluded that the zig pattern along 50° of feed direction would be the strategy leading to increased absolute stability for the down milling mode at 50% radial depth of cut. Overall, the absolute stability limit can be increased from 0.1 to 0.16 mm by adjusting the feed direction, which in return leads to 33% of time saving if the cutting depth is set at the absolute stability limit. Even more time saving can be achieved as the common stability pocket is considered, which provides 0.25 mm of stability limit around 3600 rpm.

6.1.2 Evaluation of the default milling tool path patterns

The default milling tool path patterns are compared in terms of the absolute stability index. In order to keep the same cutting mode, i.e., down milling, throughout the tool path, only the zig and follow periphery patterns are considered. The zig pattern is applied in two main feed directions, i.e., 0° and 90°. Thus, the tool path patterns under consideration are named as ZIG0, ZIG90, and FP. The local feed rate directions corresponding to these patterns are depicted in Fig. 10.

The stability lobes around the 3300 rpm of spindle speed are calculated at all robot positions using the corresponding feed directions, as plotted on top of each other in Fig. 11. It is seen that due to variation of the tool tip FRFs with the robot position, the stability lobes shift both horizontally and

Fig. 10 The local feed rate directions for the default patterns. **a** Zig pattern (0°). **b** Zig pattern (90°). (c) Follow periphery pattern

(a) Zig pattern (0°)

(b) Zig pattern (90°)

(c) Follow periphery pattern
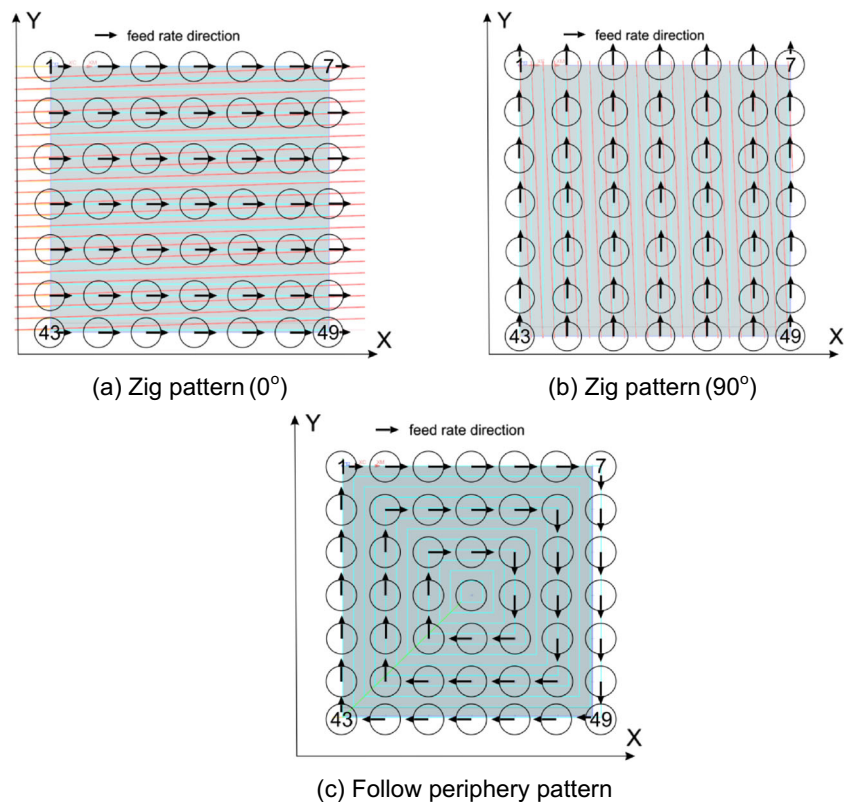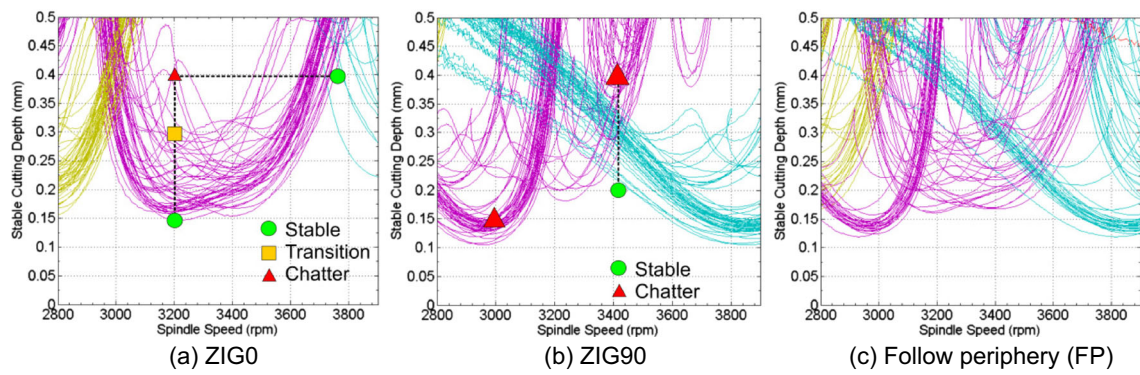
Fig. 11 Stability diagrams for the default milling patterns. **a** ZIG0. **b** ZIG90. **c** FP

vertically. As a result, the area of the common stability pocket varies significantly.

In Fig. 11a, the stability diagrams generated for the ZIG0 pattern are plotted, where the lobes show a good grouping behavior resulting in relatively wider stability pockets. However, the FP pattern is considered in Fig. 11c; there is almost no common stability pocket. In this study, the relation of stability pockets with the feed rate directions is only studied through default tool path patterns. However, determination of an optimum tool path pattern requires an optimization technique that considers the combinatorial relation between the feed rate directions at all robot positions.

The variation of the absolute stability limits, corresponding to each milling pattern, throughout the workspace is plotted in Fig. 12, where it is seen that the ZIG0 pattern results in better absolute stability compared to the other two, i.e., ZIG90 and FP. The optimized milling pattern results in minimum and maximum absolute stability limits of 0.158 and 0.358 mm, respectively, depending on the robot position. The minimum and maximum absolute stability limits for the ZIG0 pattern are 0.147 and 0.295 mm, respectively. The ZIG90 pattern leads to
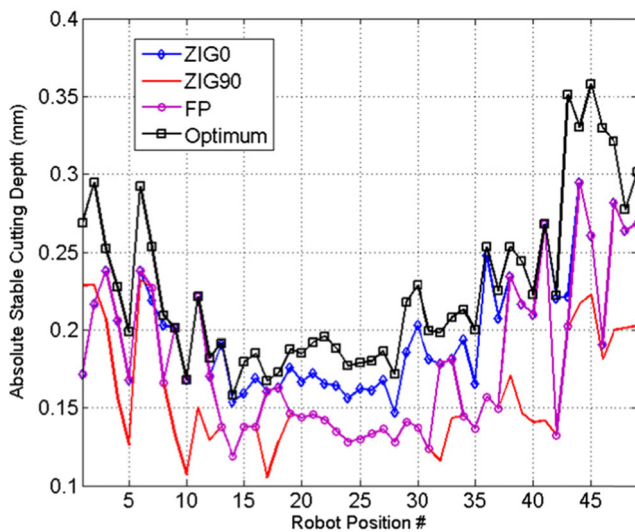
the worst absolute stability at most of the robot positions. The comparison of the default milling patterns is given in Table 1.

6.2 Experimental demonstration

In this section, the simulations are experimentally validated by performing representative machining tests using the ZIG0 and ZIG90 patterns, where the spindle speed and cutting depth are selected according to the stability lobes given in Fig. 11a, b. It is aimed at demonstrating that the simulations are accurate enough to select the appropriate tool path pattern for the case study. In the experiments, it is aimed to verify the tool path pattern selection both based on the absolute stability limit and the stability pockets. The spindle speed and cutting depth are listed in Table 2, which are marked on panels a and b of Fig. 11, respectively, as well. The FFT of the vibration data collected in the feed direction is plotted in Fig. 13.

The comparison of panels a, b, and c of Fig. 13 shows that the absolute stability limit was predicted accurately for the ZIG0 pattern. The tooth passing frequency, ω_t, is 111 Hz, whereas the chatter frequency, ω_c, rises around 500 Hz, which is in between the fourth and fifth multiples of the tooth passing frequency. Then, a comparison of panels c and e of Fig. 13 shows that the prediction of the maximum stability with the lobbing effect is reasonably accurate. As the ZIG90 pattern is considered, it is experimentally shown that the absolute stability limit is lower than 0.15 mm, which was predicted to be 0.1 mm. The maximum stability limit achieved in the experiments was 0.2. At 3420 rpm, the test at 0.4 mm depth demonstrated chatter frequency around 511 Hz (see Fig. 13g), whereas the test at 0.2 mm depth was clear of any chatter

Fig. 12 The stability lobes and absolute stability limits for each milling pattern

Table 1 Comparison of milling patterns in terms of absolute stability limits

	Optimized	ZIG0	ZIG90	Follow periphery
Min a_{abs} (mm)	0.158	0.147	0.105	0.119
Max a_{abs} (mm)	0.358	0.295	0.229	0.295
ASI (%)	100	89	69	79

Table 2 Experiment conditions

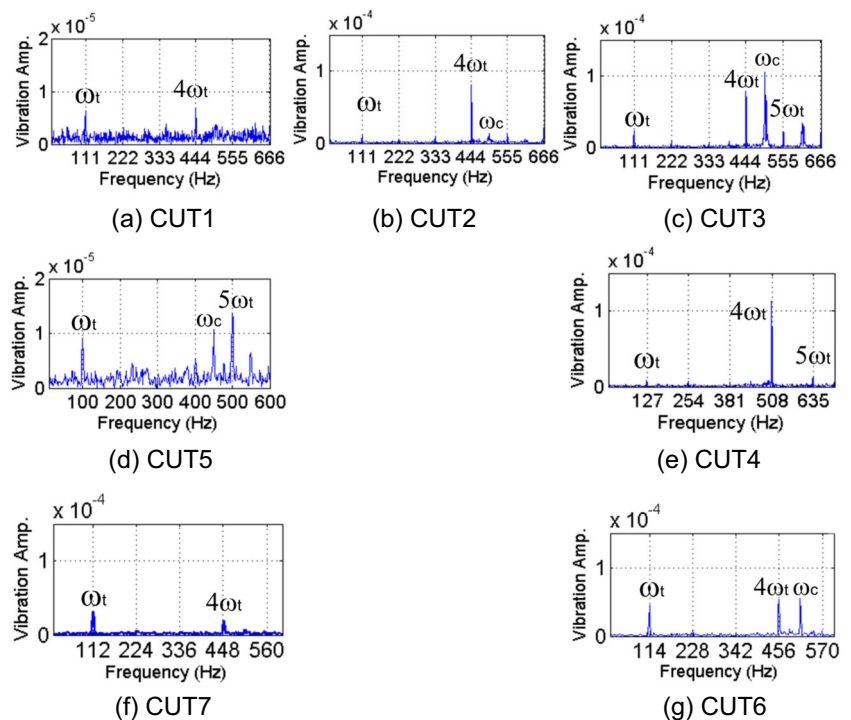|	Pattern	Cutting depth (mm)	Spindle speed (rpm)	Selection criteria	Condition
Cut 1	ZIG0	0.15	3330	Absolute stability	Stable
Cut 2	ZIG0	0.3	3330	Absolute stability	Marginal
Cut 3	ZIG0	0.4	3330	Absolute stability	Chatter
Cut 4	ZIG0	0.4	3800	Stability pocket	Stable
Cut 5	ZIG90	0.15	3000	Absolute stability	Chatter
Cut 6	ZIG90	0.4	3420	Stability pocket	Chatter
Cut 7	ZIG90	0.2	3420	Stability pocket	Stable

frequency as shown in Fig. 13f. The experimental verification also showed that ZIG0 leads to a 50% increase in absolute stability limits compared to ZIG90, whereas there is around 100% increase in the maximum stability limit, which can be achieved in the stability pockets.

7 Conclusions

This paper presents an approach to evaluate and select tool path patterns for increased chatter-free MRR in robotic milling. The machining area is divided into number of distinct points. Then, the optimal feed direction is decided based on the maximum absolute stability at each region considering the asymmetrical and position-dependent tool tip dynamics. It is shown that the feed direction leading to the maximum stability is significantly affected by the asymmetrical and position-dependent tool tip dynamics due to the modes introduced by the robotic structure. Due to the directional effects and positional dependency, the optimum feed direction becomes a function of the radial depth of cut and robot position, respectively. In the case study, it is shown that the presented approach can be used to select the tool path pattern and feed direction either locally or globally. It is also demonstrated that selection of the local feed direction based on absolute stability may not always lead to the maximum stability limit due to the stability pockets. This is mainly because the location of the stability pockets depends on the feed direction, as well. By proper selection of the machining strategies, the absolute stability can be increased by around 50%, whereas the maximum stability limit can be increased up to 100%. The presented approach has potential to be applied on five-axis surface milling once it is integrated with a five-axis milling process model, which can predict the stability limits in five-axis milling. Selection of local feed directions considering the location of stability lobes requires a recursive combinatorial optimization approach such as dynamic programming, which can be considered as a future extension of the current study.

Fig. 13 FFT of the vibration data to assess milling stability. **a** Cut 1. **b** Cut 2. **c** Cut 3. **d** Cut 5. **e** Cut 4. **f** Cut 7. **g** Cut 6

References

1. Zaeh MF, Roesch O (2014) Improvement of the machining accuracy of milling robots. Prod Eng 8(6):737–744
2. Munoa J, Beudaert X, Dombovari Z, Altintas Y, Budak E, Brecher C, Stepan G (2016) Chatter suppression techniques in metal cutting. CIRP Annals-Manufacturing Technology 65(2):785–808
3. Budak E (2006) Analytical models for high performance milling. Part II: process dynamics and stability. International Journal of Machine Tool & Manufacture 46:1489–1499
4. Munoa J, Dombovari Z, Mancisidor I, Yang Y, Zatarain M (2013) Interaction between multiple modes in milling processes. Mach Sci Technol 17(2):165–180
5. Tunc, L.T. and Shaw, J. 2015 Experimental study on investigation of dynamics of hexapod robot for mobile machining. The International Journal of Advanced Manufacturing Technology, pp.1–14
6. Tunc, L.T. and Shaw, J. 2016 Investigation of the effects of Stewart platform-type industrial robot on stability of robotic milling. The International Journal of Advanced Manufacturing Technology, pp.1–11
7. Feng HY, Su N (2000) Integrated tool path and feed rate optimization for the finishing machining of 3D plane surfaces. International Journal of Machine Tools & Manufacture 40:1557–1572
8. Ramos AM, Relvas C, Simoes JA (2003) The influence of finishing milling strategies on texture, roughness and dimensional deviations on the machining of complex surfaces. J Mater Process Technol 136(1):209–216
9. Toh CK (2004) A study of the effects of cutter path strategies and orientations in milling. J Mater Process Technol 152:346–335
10. Monreal M, Rodrigues CA (2003) Influence of tool path strategy on cycle time of high speed milling. Compter-Aided Design 35:395–401
11. Giri V, Bezbaruah D, Bubna P, Choudhury AR (2005) Selection of master cutter paths in sculptured surface machining by employing curvature principle. Int J Mach Tools Manuf 45(10):1202–1209
12. Quinsat Y, Sabourin L (2007) Optimal selection of machining direction for three-axis milling of sculptured parts. Int J Adv Manuf Technol 33(7–8):684–692
13. Bohez, E.L., Makhanov, S.S., Munlinb, M., Phien, H.N. and Tabucanon, M.T. 2009 On 5-axis freeform surface machining optimization: vector field clustering approach. International Journal of CAD/CAM, 5(1)
14. Lim EM, Menq CH (1997) Integrated planning for precision machining of complex surfaces. Part 1: cutting-path and feed rate optimization. Int J Mach Tools Manuf 37(1):61–75
15. De Lacalle LL, Lamikiz A, Sanchez JA, Salgado MA (2007) Toolpath selection based on the minimum deflection cutting forces in the programming of complex surfaces milling. Int J Mach Tools Manuf 47(2):388–400
16. Lazoglu I, Manav C, Murtezaoglu Y (2009) Tool path optimization for free form surface machining. CIRP Annals-Manufacturing Technology 58(1):101–104
17. Manav C, Bank HS, Lazoglu I (2013) Intelligent toolpath selection via multi-criteria optimization in complex sculptured surface milling. J Intell Manuf 24(2):349–355
18. Pan Z, Zhang H, Zhu Z, Wang J (2006) Chatter analysis of robotic machining process. J Mater Process Technol 173:301–309
19. Zaghbani I., Songmene V., Bonev I., 2013, An experimental study on the vibration response of a robotic machining system. Proceedings of the Institution of Mechanical Engineers. Part B: Journal of Engineering Manufacture, 227/6:866–880.
20. Abele E, Weigold M, RothenBücher S (2007) Modelling and identification of an industrial robot for machining applications. CIRP Ann 56:387–390
21. Olabi A, Béarée R, Gibaru O, Damak M (2010) Feedrate planning for machining with industrial six-axis robots. Control Eng Pract 18(5):471–482
22. Budak E, Altintas Y (1995) Analytical prediction of stability lobes in milling. CIRP Ann 44/1:357–362
23. Law M., Phani AS., Altintas, Y. 2013 Position-dependent multibody dynamic modeling of machine tools based on improved reduced models. ASME Journal of Manufacturing Science and Engineering Vol: 135–2
24. Budak E, Tekeli A (2005) Maximizing chatter free material removal rate in milling through optimal selection of axial and radial depth of cut pairs. CIRP Annals-Manufacturing Technology 54(1):353–356